LETTER SCIENCE CHINA Materials

mater.scichina.com link.springer.com

Published online 10 January 2018 | https://doi.org/10.1007/s40843-017-9186-3
Sci China Mater 2018, 61(5): 752–757

A europium(III) metal-organic framework as ratiometric turn-on luminescent sensor for Al^{3+} ions

Xinhui Zhou[1*], Jiahui Cheng[1], Liang Li[1], Qiang Chen[1], Yujian You[1], Hongping Xiao[2] and Wei Huang[1,3*]

In recent years, luminescent metal–organic frameworks (MOFs) as a new type of sensing material are receiving enormous attention for their superior performance in chemical sensors and biosensors [1–2]. Taking account of the excellent optical properties such as large Stokes shifts and high color purity of lanthanide MOFs (LnMOFs), a great deal of important investigations on LnMOFs have been carried out. And then, their promising abilities in detecting temperature, metal ions, oxygen, explosives and polychlorizated benzenes with high sensitivity and selectivity have also been exploited successfully [3–22]. Ratiometric luminescent sensors can provide a self-calibrated analyte concentration readout, which is unaffected by fluctuations of sensor concentration and/or instrumental parameters. However, it is noticed that a majority of related reports are limited to the detection of analyte using single emission, although ratiometric sensors based on dual-emission are more reliable and accurate than the sensors based on single emission. For ratiometric sensors, not only are two significantly different emissions necessary, but two emissions need distinctive response to the analyte. From this point of view, LnMOFs with ligand and Ln^{3+} emissions are very attractive, because organic ligands and Ln^{3+} ions as the luminescent centers possess completely different physical and chemical properties and they would produce different interactions with analytes. Thus, LnMOFs have been extensively applied to construct ratiometric sensors recently [3,22].

Aluminium exists in soil, containers and structural materials, which may release Al^{3+} due to the corrosion and/or dissolvation, inducing the increasing risk of Al^{3+} absorption by the human body [23–27]. However, excessive Al^{3+} in human body may cause damage to nucleic acids and proteins or the central nervous system [28–30]. Thus, it is important to detect Al^{3+} with high selectivity and sensitivity, both in the environment and organisms [31,32]. As far as we are concerned, few LnMOFs display high selectivity and sensitivity for Al^{3+} [33–35]. It is noted that Al^{3+} may replace the Ln^{3+} in the framework or interact with the ligands [36]. As a consequence, both ligand and Ln^{3+} emissions may be interfered by Al^{3+} ions. These facts impel us to realize LnMOFs ratiometric sensors for Al^{3+} by the judicious choice of the organic ligand. Recently, a few works reported different fluorescence response behavior to Al^{3+} ions for the emissions of the ligand and Tb^{3+} ion [37,38]. In these cases, the Tb^{3+} emission decreases gradually, whereas the ligand emission shows a strong enhancement as the addition of Al^{3+} ions. Inspired by these cases, we aimed to synthesize LnMOFs as ratiometric luminescent sensors to detect Al^{3+} ions.

In this work, three Ln-MOFs, $(Me_2NH_2)[Ln_2L_2(NO_3)_2(\mu_3\text{-}OH)(H_2O)]\cdot 2H_2O\cdot 2DMA$, [Ln=Eu(**1**), Gd(**2**) and Tb(**3**), DMA=dimethylacetamide], were obtained based on a robust ligand, 9-methyl-9-hydroxy-fluorene-2,7-dicarboxylic acid (H_2L), which can effectively transfer energy to Eu^{3+} by antenna effect. All frameworks are isostructural, and the topology analysis of frameworks shows a uninodal 8-connected body centered cubic (bcu) network. The luminescence investigations reveal that **1** is a LnMOF ratiometric sensor for Al^{3+} with high sensitivity and selectivity.

Compounds **1**–**3** were synthesized in the mixed sol-

[1] Key Laboratory for Organic Electronics and Information Displays & Jiangsu Key Laboratory for Biosensors, Institute of Advanced Materials (IAM), Jiangsu National Synergetic Innovation Center for Advanced Materials (SICAM), Nanjing University of Posts & Telecommunications, Nanjing 210023, China
[2] College of Chemistry and Materials Engineering, Wenzhou University, Wenzhou 325035, China
[3] Key Laboratory of Flexible Electronics (KLOFE) & Institute of Advanced Materials (IAM), Jiangsu National Synergetic Innovation Center for Advanced Materials (SICAM), Nanjing Tech University, Nanjing 211816, China
* Corresponding authors (emails: iamxhzhou@njupt.edu.cn (Zhou X); iamwhuang@njtech.edu.cn (Huang W))

vents under solvothermal conditions. Due to the poor crystal qualities, X-ray single-crystal diffraction data for **2** were not obtained. However, powder X-ray diffraction (PXRD) data, thermogravimetric analysis (TG) and infrared spectroscopy (IR) confirm that **2** is isostructural with **1** and **3** (Figs S1–S3). They are stable in air but unstable in water, and their stabilities in dimethylformamide (DMF), ethyl acetate (EA), ethyl alcohol (EtOH), *N*-methyl pyrrolidone (NMP) are also verified by PXRD of **1** dipped in these solvents for 24 h. As shown in Fig. S2, the presence of H_2O molecules and $-CH_3$ is confirmed by the characteristic bands of O–H (3,680–3,000 cm^{-1}) and C–H (2,900–3,000 cm^{-1}) vibrations, respectively. Since no strong absorption peaks ranging from 1,690 to 1,730 cm^{-1} for −COOH are observed, and the characteristic sharp bands of carboxylate groups appear with the maxima at 1,544 and 1,381 cm^{-1} for **1**, 1,550 and 1,384 cm^{-1} for **2**, 1,553 and 1,381 cm^{-1} for **3**, all carboxyl groups for H_2L ligands in complexes **1**–**3** should be deprotonated.

Since **1**–**3** are isostructural, **1** is selected as the representative example to describe the structure in detail. The asymmetric unit of **1** includes a L^{2-} ligand, half a coordinated H_2O, a free H_2O, half a μ_3–OH^-, a coordinated NO_3^-, a free DMA, half a free $Me_2NH_2^+$ and two crystallographically unique Eu^{3+} ions, of which Eu1 lies on the mirror plane parallel with *ab* crystal plane and Eu2 on the twofold axis parallel with *c* axis (Fig. 1a). Eu1 and Eu2 are coordinated by oxygen atoms with tricapped and bicapped trigonal prismatic coordination geometry, respectively. Four Eu^{3+} ions, two μ_3–OH^- and four carboxylate oxygens form face-sharing defective cubes-like Eu_4O_6 metal-oxygen cluster. Each L^{2-} ligand bridges two Eu_4O_6 clusters and each Eu_4O_6 cluster is coordinated by eight L^{2-} ligands (Fig. 1b). The resulting three-dimensional framework possesses rhombic channels extended along the [010] direction with 14×20 $Å^2$ diagonally dimensions in which H_2O, NO_3^-, $Me_2NH_2^+$ and DMA locate as guests and counterions (Fig. 1c, d). The solvent accessible space for **1** without these guests and counterions is 4,319 $Å^3$ per unit cell or 65% of the total volume, calculated using the PLATON routine [39]. The 3D framework can be rationalized by the TOPOS 4.0 program [40] as a uninodal 8-connected bcu topological network with a Schläfli symbol of $4^{24}.6^4$ by considering the Eu_4O_6 clusters as 8-connected nodes and L^{2-} ligands as linkers, respectively.

Powder **1**–**3** were heated up to 800°C in N_2 atmosphere at a heating rate of 10°C min^{-1}. The TG curves show that **1**–**3** undergo similar weight loss processes (Fig. S3). In the

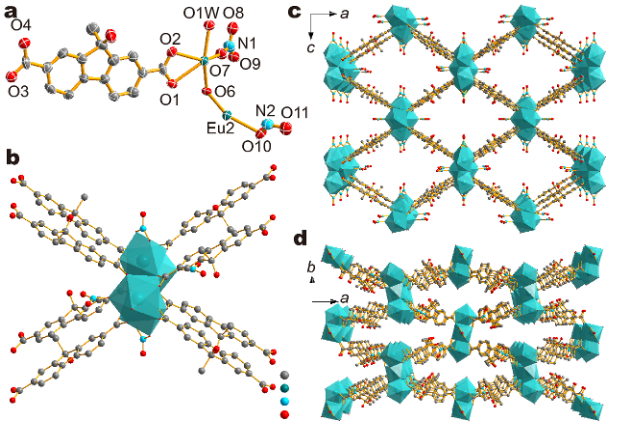

Figure 1 (a) View of the asymmetric unit of **1** with the thermal ellipsoids drawn at the 50% probability level. (b) View of Eu_4O_6 metal-oxygen cluster. View of crystal structure of **1** along the *b*-axis (c) and *c*-axis (d). All hydrogen atoms, $Me_2NH_2^+$, uncoordinated water and DMA molecules are omitted for clarity.

temperature range of 20–110°C, the weight losses of **1**–**3** are 3.9%, 2.3% and 2.2%, respectively, corresponding to the departure of all water molecules for **1** and two lattice water molecules for **2** and **3** (calc. 4.2%, 2.8%, 2.8%). The weight loss of 16.5%, 19.1% and 18.3% in the range of 110–245°C for **1**–**3** is attributed to the departure of two DMA, a $Me_2NH_2^+$ for **1**, two DMA, a $Me_2NH_2^+$ and a coordinated water molecule for **2** and **3** (calc. 17.2%, 18.5%, 18.3%). Further heating leads to the decomposition of ligand molecules. The PXRD patterns of **1**–**3** are shown in Fig. S1. The experimental XRD patterns of the synthesized **1**–**3** are in good agreement with the simulated, showing the good phase purity.

The photoluminescence spectra of **1**–**3** in solid state are shown in Fig. S4a. Upon excitation at 335 nm, the emission spectrum of **1** reveals a weak emission band with intensity maximum at 362 nm ($S_1 \rightarrow S_0$ transition), and characteristic emission peaks of Eu^{3+} at 596 ($^5D_0 \rightarrow {}^7F_1$ transition) and 620 nm ($^5D_0 \rightarrow {}^7F_2$ transition). The decay curve of the $^5D_0 \rightarrow {}^7F_2$ transition of **1** was best fitted by a second order exponential function with lifetimes τ_1 = 302.54 μs (α_1 = 3.95%) and τ_2 = 771.67 μs (α_2 = 96.05%) (Fig. S4b). Quantum yield of **1** is 40.6%. **2** exhibits a ligand-based emission centered at 368 nm. The triplet state energy (T_1) and the singlet state energy (S_1) of ligand are estimated as 20,533 cm^{-1} and 25,974 cm^{-1} from the 77 K phosphorescence spectrum (Fig. S5) and the absorption spectrum (Fig. S6) of **2**. **3** exhibits a strong ligand-based emission band centered at 365 nm and weak characteristic emission peaks of Tb^{3+} ions at 494 and 550 nm. The blue-shift of ligand-centered emission ob-

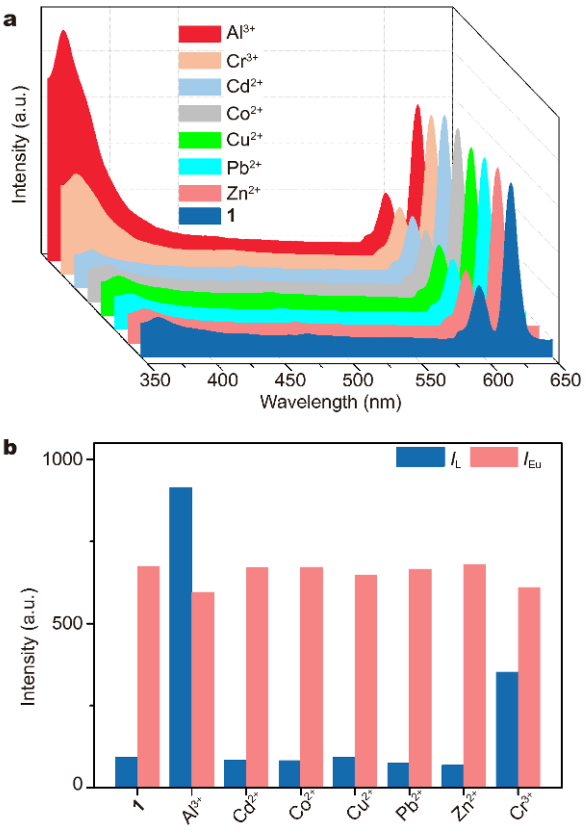

Figure 2 (a) Upon excitation at 335 nm, the photoluminescence spectra of **1** treated with different metal ions (1×10^{-4} mol L^{-1}) in DMF and (b) the corresponding emission intensities of $^5D_0\rightarrow{}^7F_2$ transition (I_{Eu}, 620 nm) and $S_1\rightarrow S_0$ (I_L, 362 nm) of **1**.

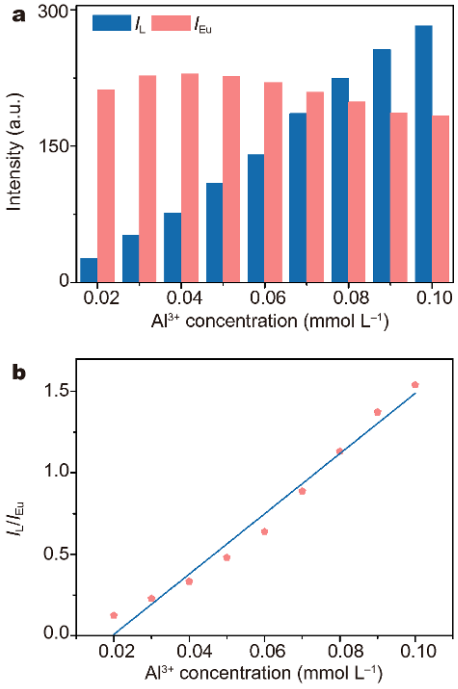

Figure 3 I_L(362 nm) and I_{Eu}(620 nm) (a), and the intensity ratio of I_L to I_{Eu} (b) of **1** treated in different concentrations of Al^{3+} in DMF.

served for **1**–**3**, compared to that of H_2L itself [13] (412 nm), may be attributed to the torsion of ligand when coordinating to the metal ion.

The excellent luminescence property of **1** promoted us to develop its ability as luminescent sensing material. Detection of various metal ions (Cd^{2+}, Co^{2+}, Cu^{2+}, Pb^{2+}, Zn^{2+}, Al^{3+} and Cr^{3+}) was performed by collecting the change in fluorescence spectra of **1** suspension in DMF (3 mg per 3 mL) before and after addition of the metal ions with the concentration of 1×10^{-4} mol L^{-1}. The luminescent spectra are shown in Fig. 2. The results reveal that most metal ions do not show obvious change on luminescence intensity for both the ligand-centered emission and Eu^{3+} ion emission. However, among the metal ions studied, the influence of Cr^{3+} and Al^{3+} ions on the emissions of **1** are highly pronounced, particularly for Al^{3+} ions, suggesting that **1** possesses a good luminescent sensing selectivity for Al^{3+} ions. The Al^{3+} ion increases dramatically the ligand-centered emission intensity by approximately 880% simultaneously with a subtle change in Eu^{3+} ion emission intensity.

To have a better understanding of the luminescence response of **1** to Al^{3+} ions, photoluminescence titration experiments were further conducted. As the concentrations of Al^{3+} increase from 0.2×10^{-4} to 1×10^{-4} mol L^{-1}, the ligand-centered emission intensities progressively increase whereas the Eu^{3+} ion emission keeps almost constant (Fig. 3a). The intensity of emission at 620 nm is seven times higher than that at 362 nm without the presence of Al^{3+} ions. However, when the concentration of the Al^{3+} ions reaches 1×10^{-4} mol L^{-1}, the intensity of emission at 362 nm is 1.6 times bigger than that at 620 nm. Ratiometric luminescent sensors based on dual-emission provide a self-calibrated data readout, and are more reliable and accurate than those based on a single emission intensity. In this work, the intensity ratio of emissions at 362 and 620 nm changes with the Al^{3+} ion concentration, which encourage us to check whether or not **1** can be used as ratiometric luminescent sensor for the detection of Al^{3+} ions. So we carefully examined the photoluminescence titration experimental data and tried to find the law of relationship between the emission intensity ratio of $S_1\rightarrow S_0$ (I_L) to $^5D_0\rightarrow{}^7F_2$ transition (I_{Eu}) and Al^{3+} ion concentration. As shown in Fig. 3b, the Al^{3+} ion

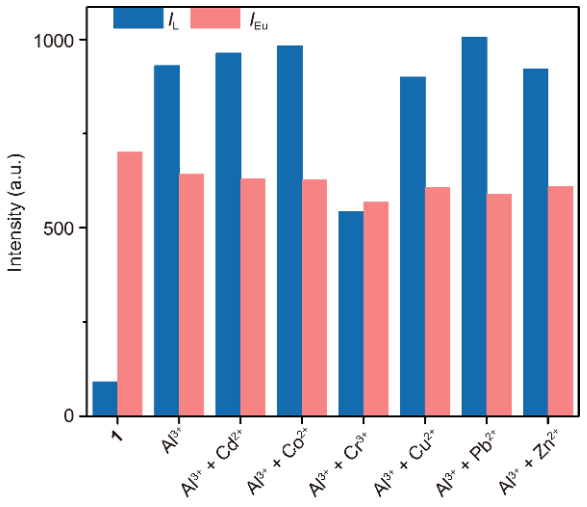

Figure 4 The I_L(362 nm) and I_{Eu}(620 nm) of **1** treated in mixed metal ions.

concentration can be linearly related to I_L/I_{Eu} by the equation $I_L/I_{Eu} = k[Al^{3+}]$–0.36 (k=18,502 L mol^{-1}, R^2 = 0.98), from 0.2×10^{-4} to 1×10^{-4} mol L^{-1}. The limit of detection of **1** for Al^{3+} ions is calculated as 1.30×10^{-6} mol L^{-1}, indicating that **1** is an excellent candidate of the ratiometric luminescent Al^{3+} ion sensor. In addition, we have investigated the recyclability of sensing performance of **1**. Unfortunately, this material shows a poor recyclability for sensing performance (Fig. S7).

The high selectivity of **1** for Al^{3+} sensing was further confirmed by competitive experiments, which was conducted by adding a interferential metal ion (1×10^{-4} mol L^{-1}) into the **1** suspension containing 1×10^{-4} mol L^{-1} Al^{3+} in DMF. As shown in Fig. 4, the ligand-based emission exhibits similar degree of enhancement with a subtle change in Eu^{3+} ion emission intensity before and after introduction of Cd^{2+}, Co^{2+}, Cu^{2+}, Pb^{2+} or Zn^{2+}, suggesting that these metal ions in solution would not influence the detection for Al^{3+}. However, for Cr^{3+} ions, a smaller enhancement in the ligand-based emission was observed, revealing that the detection for Al^{3+} can be interfered by Cr^{3+} because Cr^{3+} and Al^{3+} possess +3 charge while other metal ions possess +2 charge and the radius of Cr^{3+} (0.0615 nm) is closer to that of Al^{3+} (0.0535 nm) relative to that of other metal ions (>0.065 nm).

According to previous reports, the enhancement effect on ligand-based fluorescence of MOFs by Al^{3+} or Cr^{3+} may be attributed to the following factors: (a) cation-exchange between Ln^{3+} of framework and Al^{3+} or Cr^{3+} and (b) interaction between ligand and Al^{3+} or Cr^{3+}. Several Al^{3+} sensors of MOF materials based on the former have been reported. The first example was described in 2013 by Sun *et al.* [30], who used compound $[H_2N(CH_3)_2][Eu(H_2O)_2(BTMIPA)]\cdot 2H_2O$ (H_4BTMIPA = 5,5'-methylenebis(2,4,6-trimethylisophthalic acid)) to detect the Al^{3+}. The authors observed that ligand emission increased and the compounds dissolved gradually leading to the clear solution due to Al^{3+} substituting Ln^{3+} in the framework when Al^{3+} concentration was greater than 0.001 mol L^{-1} and the framework of the compound collapsed completely when the Al^{3+} concentration reached 0.01 mol L^{-1}. However, we found that **1** suspension in DMF containing Al^{3+} kept turbid and strong characteristic red light emission of Eu^{3+} ions after **1** dipped in DMF containing 1×10^{-4} mol L^{-1} and 1×10^{-5} mol L^{-1} Al^{3+} for 12 h, respectively, as shown in Fig. S8, which indicate that cation-exchange do not contribute to ligand-based fluorescence enhancement in this work. So, we speculated that the interactions between ligand and Al^{3+} or Cr^{3+} lead to the ligand-based fluorescence enhancement, and the luminescence spectra of the H_2L (9-methyl-9-hydroxy-fluorene-2,7-dicarboxylic acid) and H_2MFDC (9,9'-dimethyl-fluorene-2,7-dicarboxylic acid) solutions in DMF before and after addition of Al^{3+} or Cr^{3+} (1×10^{-4} mol L^{-1}) were investigated. The H_2L and H_2MFDC are two very similar ligands with a marginal difference, a methyl and a hydroxy on 9-position for H_2L, two methyl on 9-position for H_2MFDC. As shown in Figs S9 and S10, when Al^{3+} or Cr^{3+} was added to the solution, the emission intensity of H_2L increases while the intensity of H_2MFDC remains unchanged. It is a very powerful suggestion that the interactions between the hydroxyl on the 9-position of H_2L and Al^{3+} or Cr^{3+} are the essential factor for ligand-based fluorescence enhancement. Furthermore, the enhancement effect is more pronounced for the LnMOF **1** than free H_2L, illustrating that the coordination between Eu^{3+} and H_2L plays the important role in signal amplification. Based on the above results, we proposed that the hydroxyl on the 9-position of ligand in the **1** interacts with Al^{3+} or Cr^{3+} to reduce the vibration of O–H, which effectively inhibits nonradiative S_1 transition and results in the ligand emission enhancement.

In summary, we have obtained three isostructural LnMOFs (Eu(**1**), Gd(**2**), Tb(**3**)) based on 9-methyl-9-hydroxy-fluorene-2,7-dicarboxylic acid (H_2L). In **1**–**3**, the face-sharing defective cubes-like Eu_4O_6 metal-oxygen clusters as 8-connected nodes construct the body centered cubic topological network with a Schläfli symbol of $4^{24}.6^4$. The unique luminescence feature gives **1** the ability to detect the Al^{3+} ions by the ratiometric luminescent

approach with slope of 18,502 mol L^{-1}. We have also demonstrated that interactions between the –OH on the 9-position of ligand and Al^{3+} ions contribute to the sensing behavior. Our future work will be continually focused on the development and optimization of ratiometric luminescent sensors for other toxic metal ions.

Received 23 October 2017; accepted 19 December 2017; published online 10 January 2018

1 Allendorf MD, Bauer CA, Bhakta RK, *et al.* Luminescent metal–organic frameworks. Chem Soc Rev, 2009, 38: 1330–1352
2 Cui Y, Yue Y, Qian G, *et al.* Luminescent functional metal–organic frameworks. Chem Rev, 2012, 112: 1126–1162
3 Rocha J, Brites CDS, Carlos LD. Lanthanide organic framework luminescent thermometers. Chem Eur J, 2016, 22: 14782–14795
4 Li L, Zhu Y, Zhou X, *et al.* Visible-light excited luminescent thermometer based on single lanthanide organic frameworks. Adv Funct Mater, 2016, 26: 8677–8684
5 Cui Y, Xu H, Yue Y, *et al.* A luminescent mixed-lanthanide metal–organic framework thermometer. J Am Chem Soc, 2012, 134: 3979–3982
6 Cui Y, Song R, Yu J, *et al.* Dual-emitting mof⊃dye composite for ratiometric temperature sensing. Adv Mater, 2015, 27: 1420–1425
7 Hu Z, Deibert BJ, Li J. Luminescent metal–organic frameworks for chemical sensing and explosive detection. Chem Soc Rev, 2014, 43: 5815–5840
8 Li L, Chen Q, Niu Z, *et al.* Lanthanide metal–organic frameworks assembled from a fluorene-based ligand: selective sensing of Pb^{2+} and Fe^{3+} ions. J Mater Chem C, 2016, 4: 1900–1905
9 Liu B, Hou L, Wu WP, *et al.* Highly selective luminescence sensing for Cu^{2+} ions and selective CO_2 capture in a doubly interpenetrated MOF with Lewis basic pyridyl sites. Dalton Trans, 2015, 44: 4423–4427
10 Hao JN, Yan B. A water-stable lanthanide-functionalized MOF as a highly selective and sensitive fluorescent probe for Cd^{2+}. Chem Commun, 2015, 51: 7737–7740
11 Dou Z, Yu J, Cui Y, *et al.* Luminescent metal–organic framework films as highly sensitive and fast-response oxygen sensors. J Am Chem Soc, 2014, 136: 5527–5530
12 Hu Z, Tan K, Lustig WP, *et al.* Effective sensing of RDX *via* instant and selective detection of ketone vapors. Chem Sci, 2014, 5: 4873–4877
13 Li A, Li L, Lin Z, *et al.* Guest-induced reversible structural transitions and concomitant on/off luminescence switching of an Eu(III) metal–organic framework and its application in detecting picric acid. New J Chem, 2015, 39: 2289–2295
14 Wang L, Fan G, Xu X, *et al.* Detection of polychlorinated benzenes (persistent organic pollutants) by a luminescent sensor based on a lanthanide metal–organic framework. J Mater Chem A, 2017, 5: 5541–5549
15 Cheng T, Hu J, Zhou C, *et al.* Luminescent metal-organic frameworks for nitro explosives detection. Sci China Chem, 2016, 59: 929–947
16 Zhou J, Li H, Zhang H, *et al.* A bimetallic lanthanide metal-organic material as a self-calibrating color-gradient luminescent sensor. Adv Mater, 2015, 27: 7072–7077
17 Zhang SY, Shi W, Cheng P, *et al.* A mixed-crystal lanthanide zeolite-like metal–organic framework as a fluorescent indicator for lysophosphatidic acid, a cancer biomarker. J Am Chem Soc, 2015, 137: 12203–12206
18 Zhao M, Yuan K, Wang Y, *et al.* Metal–organic frameworks as selectivity regulators for hydrogenation reactions. Nature, 2016, 539: 76–80
19 He L, Liu Y, Liu J, *et al.* Core-shell noble-metal@metal-organic-framework nanoparticles with highly selective sensing property. Angew Chem Int Ed, 2013, 52: 3741–3745
20 Wang T, Jia Y, Chen Q, *et al.* A new luminescent metal-organic framework for selective sensing of nitroaromatic explosives. Sci China Chem, 2016, 59: 959–964
21 Wang S, Ma R, Chen Z, *et al.* Solvent- and metal-directed lanthanide-organic frameworks based on pamoic acid: observation of slow magnetization relaxation, magnetocaloric effect and luminescent sensing. Sci China Chem, 2016, 59: 948–958
22 Li B, Wen HM, Cui Y, *et al.* Emerging multifunctional metal-organic framework materials. Adv Mater, 2016, 28: 8819–8860
23 Zhao M, Deng Z, Tang J, *et al.* 2-(1-Pyrenyl) benzimidazole as a ratiometric and "turn-on" fluorescent probe for iron(III) ions in aqueous solution. Analyst, 2016, 141: 2308–2312
24 Gupta VK, Jain AK, Maheshwari G. Aluminum(III) selective potentiometric sensor based on morin in poly(vinyl chloride) matrix. Talanta, 2007, 72: 1469–1473
25 Deng M, Wang S, Liang C, *et al.* A FRET fluorescent nanosensor based on carbon dots for ratiometric detection of Fe^{3+} in aqueous solution. RSC Adv, 2016, 6: 26936–26940
26 Patidar R, Rebary B, Bhadu GR, *et al.* Fluorescent carbon nanoparticles as label-free recognizer of Hg^{2+} and Fe^{3+} through effective fluorescence quenching in aqueous media. J Lumin, 2016, 173: 243–249
27 Diao Q, Ma P, Lv L, *et al.* A water-soluble and reversible fluorescent probe for Al^{3+} and F^- in living cells. Sensor Actuat B-Chem, 2016, 229: 138–144
28 Pithadia AS, Lim MH. Metal-associated amyloid-β species in Alzheimer's disease. Curr Opin Chem Biol, 2012, 16: 67–73
29 Gauthier E, Fortier I, Courchesne F, *et al.* Aluminum forms in drinking water and risk of Alzheimer's disease. Environ Res, 2000, 84: 234–246
30 Flaten TP. Aluminium as a risk factor in Alzheimer's disease, with emphasis on drinking water. Brain Res Bull, 2001, 55: 187–196
31 Fu Y, Jiang XJ, Zhu YY, *et al.* A new fluorescent probe for Al^{3+} based on rhodamine 6G and its application to bioimaging. Dalton Trans, 2014, 43: 12624–12632
32 Afshani J, Badiei A, Lashgari N, *et al.* A simple nanoporous silica-based dual mode optical sensor for detection of multiple analytes (Fe^{3+} , Al^{3+} and CN^-) in water mimicking XOR logic gate. RSC Adv, 2016, 6: 5957–5964
33 Xu XY, Yan B. Eu(III)-functionalized MIL-124 as fluorescent probe for highly selectively sensing ions and organic small molecules especially for Fe(III) and Fe(II). ACS Appl Mater Interfaces, 2015, 7: 721–729
34 Dong XY, Wang R, Wang JZ, *et al.* Highly selective Fe^{3+} sensing and proton conduction in a water-stable sulfonate–carboxylate Tb–organic-framework. J Mater Chem A, 2015, 3: 641–647
35 Liang YT, Yang GP, Liu B, *et al.* Four super water-stable lanthanide–organic frameworks with active uncoordinated carboxylic and pyridyl groups for selective luminescence sensing of Fe^{3+}. Dalton Trans, 2015, 44: 13325–13330

36 Chen Z, Sun Y, Zhang L, *et al.* A tubular europium–organic framework exhibiting selective sensing of Fe^{3+} and Al^{3+} over mixed metal ions. Chem Commun, 2013, 49: 11557–11559
37 Cao LH, Shi F, Zhang WM, *et al.* Selective sensing of Fe^{3+} and Al^{3+} ions and detection of 2,4,6-trinitrophenol by a water-stable terbium-based metal-organic framework. Chem Eur J, 2015, 21: 15705–15712
38 Zhang M, Han J, Wu H, *et al.* Tb-MOF: a naked-eye and regenerable fluorescent probe for selective and quantitative detection of Fe^{3+} and Al^{3+} ions. RSC Adv, 2016, 6: 94622–94628
39 Spek AL. Single-crystal structure validation with the program *PLATON*. J Appl Crystlogr, 2003, 36: 7–13
40 Blatov VA, O'Keeffe M, Proserpio DM. Vertex-, face-, point-, Schläfli-, and Delaney-symbols in nets, polyhedra and tilings: recommended terminology. CrystEngComm, 2010, 12: 44–48

Acknowledgements This work was supported by the National Natural Science Foundation of China (21271143), Priority Academic Program Development of Jiangsu Higher Education Institutions (PAPD) (YX03001), Jiangsu Province Double Innovation Talent Program (090300014001), Nanjing University of Posts & Telecommunications (NY212004).

Conflict of interest The authors declare no competing financial interest.

Supplementary information Experimental section, tables of crystallographic data and selected bond lengths and angles, diagrams of PXRD, IR, TG and additional photoluminescence spectra, can be found in online version. CCDC 1546509 and 1546510 contain the supplementary crystallographic data for this paper. These data can be obtained free of charge *via* www.ccdc.cam.ac.uk/data_request/cif.

Xinhui Zhou received his Bachelor degree from Dalian University of Technology in 2001, his Master degree from Shantou University in 2006, under the supervision of Prof. Dan Li and his PhD degree from Nanjing University in 2009, under the supervision of Prof. Jinglin Zuo. He joined the Institute of Advanced Materials (IAM), Nanjing University of Posts & Telecommunications in 2009. His research interests are focused on the MOF-based luminescent sensing materials.

Wei Huang received his PhD degree from Peking University in 1992. In 1993, he began his postdoctoral research at the National University of Singapore. In 2001, he was appointed as a chair professor of Fudan University, where he founded and chaired the Institute of Advanced Materials (IAM). In 2006, he was appointed vice president of Nanjing University of Posts & Telecommunications. In 2012, he was appointed the president of Nanjing Tech University. Now, he is the vice president of Northwestern Polytechnical University. He was elected as Academician of the Chinese Academy of Sciences in 2011. His research interests include organic/plastic materials and devices, nanomaterials, and nanotechnology.

基于含铕金属-有机框架的比率turn-on型铝离子发光传感器

周馨慧[1*], 程嘉荟[1], 李亮[1], 陈强[1], 游宇健[1], 肖洪平[2], 黄维[1,3*]

摘要 本文制备了三种同构镧系金属有机框架材料$(Me_2NH_2)[Ln_2L_2(NO_3)_2(\mu_3\text{-}OH)(H_2O)]\cdot 2H_2O\cdot 2DMA$, (Ln = Eu(**1**), Gd(**2**), Tb(**3**), H_2L = 9-甲基-9-羟基-2,7-芴二羧酸, DMA = 二甲基乙酰胺). 研究结果显示它们具有三维阴离子型框架结构, 该结构可简化为含有单一的8连接型节点的体心立方(bcu)型拓扑结构. 化合物**1**表现出基于配体的荧光发射峰以及铕离子的特征荧光发射峰. 荧光实验表明在DMF溶液中Al^{3+}会明显增强配体的荧光强度, 而对Eu^{3+}的荧光强度影响却很小, 这使得**1**成为了优秀的比率式发光Al^{3+}传感器. 在Al^{3+}浓度处于0.02–0.1 mmol L^{-1}范围内时, 配体与Eu^{3+}荧光强度的比值与Al^{3+}浓度成正比(斜率为18502 mol^{-1} L). 本文证实了配体9位的羟基与Al^{3+}之间的相互作用是引起配体荧光增强的主要原因.

